Quenching of Chlorophyll *a* Fluorescence in the Aggregates of LHCII: Steady State Fluorescence and Picosecond Relaxation Kinetics†

S. Vasil'ev,‡,§ K.-D. Irrgang,|| T. Schrötter,⊥ A. Bergmann,▽ H.-J. Eichler,▽ and G. Renger*,||

Faculty of Biology, Moscow State University, Moscow 119899, Russia, Max Volmer Institute for Biophysical Chemistry and Biochemistry, Technical University Berlin, D-10623 Berlin, Germany, Optical Institute, Technical University Berlin, D-10623 Berlin, Germany, and Institute of Physics, Humboldt University, Berlin, D-10099 Berlin, Germany

Received October 8, 1996; Revised Manuscript Received April 14, 1997⊗

ABSTRACT: The protein composition, steady state and time-resolved fluorescence emission spectra were studied in solubilized and aggregated LHCII complexes, that were prepared according to two different isolation protocols: (1) by fractionation of cation-depleted thylakoid membranes using the non-ionic detergent Triton X-100 according to the procedure of Burke et al. [(1978) *Arch. Biochem. Biophys. 187*, 252−263] or (2) by solubilization with *N*-β-dodecyl maltoside (β-DM) of photosystem II (PSII) membrane fragments in the presence of cations [Irrgang et al. (1988) *Eur. J. Biochem. 178*, 207−217]. Based on the analysis of the decay-associated emission spectra measured at 10 and 80 K five long-wavelength chlorophyll species were identified in aggregated LHCII complexes. These five forms are characterized by emission maxima at 681.5, 683, 687, 695, or 702 nm. All of these forms were found in both types of LHCII preparations but the relative amounts and temperature dependency of these species were markedly different in the aggregated LHCII complexes isolated by the two procedures. It was found that these differences cannot be simply explained by effects due to using a less mild detergent as β-DM or by an ionic influence of Ca^{2+}. Biochemical analysis of the protein composition showed that β-DM type LHCII consists of all the chlorophyll (Chl)binding proteins belonging to the antenna system of PSII except the CP29 type II gene product (CP29). In contrast, the Triton X-100-solubilized LHCII is highly depleted in CP26 (CP 29 type I gene product) and is contaminated by a variety of unidentified polypeptides. It is proposed that the aggregates of LHCII prepared using Triton X-100 acquire specific spectral and kinetic features due to interaction between the bulk of LHCII subunits and minor protein(s).

Recently considerable progress has been achieved in understanding the structure (Kühlbrandt et al., 1994) and function (Hemelrijk et al., 1992; Du et al., 1994) of LHCII.[1] There is, however, little information available on how LHCII subunits interact with each other and with the minor Chl−protein complexes [for a review see Jansson (1994)] and how excitation energy is transferred to the PSII core complexes (van Grondelle et al., 1994). Results of independent studies suggest that strong interactions occur between LHCII trimers *in vivo*, i.e. the organization resembles that of an oligomeric aggregate (Bassi et al., 1992; Garab et al., 1991). A number of studies have provided different lines of evidence that high-energy quenching (qE) arises from a reversible aggregation of LHCII and that qE provides a physiologically important regulation mechanism for adjusting photosystem II to the density of excitation energy (Horton et al., 1991, 1994).

It has been found that the fluorescence yield drastically decreases and additionally red-shifted components appear in the absorption and fluorescence emission spectra when aggregates of LHCII are formed *in vitro*. An emission band peaking at 700 nm was detected at 77 K *in vitro* (Ruban et al., 1992) and also in intact PSII attaining a quenched state (Ruban & Horton 1994). At room temperature the yield of this form was low, but it increased dramatically when the temperature was lowered (Ruban et al., 1992). Recently a more detailed investigation of the temperature dependency extended down to 4 K revealed that at least five long-wavelength emitting bands appear in the fluorescence spectra of LHCII. Each band has a unique temperature dependency and in general, the shorter wavelength components start to increase at lower temperature than do the longer wavelength bands (Ruban et al., 1995b). When the decay-associated fluorescence spectra at 77 K were analyzed, a dominating decay kinetics of 110 ps was found, which is indicative of highly efficient energy-quenching process(es) in LHCII aggregates. Three additional decay components were identified having maxima at 685, 695, and 700 nm with corresponding lifetimes of 0.36, 1.2, and 3.3 ns, respectively (Mullineaux et al., 1993). The origin of the different red-shifted emitters in the LHCII aggregates has not yet been clarified. Analysis of the time-resolved data *in vitro* led to the conclusion that the red-shifted species are not directly involved in the quenching mechanism. Presumably the

† S.V. acknowledges financial support from the Alexander von Humboldt Foundation. G.R. acknowledges support from the Deutsche Forschungsgemeinschaft and Fonds der Chemischen Industrie.

* Corresponding author. FAX: +49 30 314 21122.

‡ Moscow State University.

§ Present address: Max Volmer Institute for Biophysical Chemistry and Biochemistry, Technical University Berlin, D-10623 Berlin, Germany.

|| Max Volmer Institute, TU Berlin.

⊥ Institute of Physics, HU Berlin.

▽ Optical Institute, TU Berlin.

⊗ Abstract published in *Advance ACS Abstracts,* June 1, 1997.

[1] Abbreviations: LHCII, light-harvesting chlorophyll *a*/*b* binding protein; Chl, chlorophyll; PSII photosystem II, DAS, decay-associated emission spectrum; FWHM, full width at half-maximum; β-DM, *N*-β-dodecyl maltoside; qE, ΔpH dependent or high energy state quenching of chlorophyll fluorescence.

S0006-2960(96)02525-1 CCC: $14.00

quenching component is a special non-fluorescent pigment complex formed when LHCII becomes aggregated (Mullineaux et al., 1993; Horton et al., 1991). Alternatively a quenching complex with carotenoids could be formed (Gilmore et al., 1995; Jennings et al., 1994). Latest resonance Raman studies revealed an alteration of the LHCII trimer structure in its aggregated state (Ruban et al., 1995a).

Thus LHCII has a dynamic structure and the properties of its bound pigments can be modified by the spatial arrangement of the complex. Protein−protein interactions between trimers are of crucial relevance for the aggregation. Therefore studies of preparations with a quasinative protein environment are necessary for a detailed understanding of spectral properties of aggregated LHCII. In all studies reported so far the aggregation was performed with LHCII complexes isolated by solubilizing thylakoid membranes with Triton X-100 according to the procedure described by Burke et al. (1978). Recently an alternative method was reported (Irrgang et al., 1988) indicating that purified LHCII can be prepared from PS II membrane fragments by using the mild non-ionic detergent β-DM.

In this work we address two main problems: (i) in an attempt to clarify the nature of the long-shifted emitting bands, the protein composition and fluorescence emission properties of aggregated LHCII complexes were thoroughly analyzed, which were prepared according to two different protocols (Burke et al., 1978; Irrgang et al., 1988); and (ii) using these two types of samples time-resolved fluorescence measurements were performed at 10 K in order to minimize the influence of thermal back excitation transfer to higher energy states and to determine decay constants and spectral shapes of the long-shifted emission bands observed previously in steady state fluorescence spectra.

MATERIALS AND METHODS

The LHCII preparations were isolated from spinach following two different procedures: firstly by solubilization of cation-depleted thylakoid membranes with the non-ionic detergent Triton X-100 according to Burke et al. (1978) or secondly by solubilizing salt-washed PSII membrane fragments with β-DM in the presence of cations as described previously (Irrgang et al., 1988). The first procedure includes a high-salt precipitation step followed by solubilization of LHCII in a buffer containing 20 mM MES-NaOH, pH 6.5, 0.05% w/v β-DM, 15 mM NaCl to yield trimers. In the second protocol the pigment protein complexes are not precipitated by high salt concentrations. Aggregation of LHCII is induced by dialysing the samples for 72 h at 4 °C in the dark against a detergent-free buffer solution containing 20 mM MES-NaOH, pH 6.5, 10 mM $MgCl_2$, 5 mM NaCl. Aggregates of both types of samples used in this study were prepared from trimers by dialysis under the same conditions.

Isolated LHCII was routinely analyzed as follows: the Chl content was determined using the procedure described by Porra et al. (1989). SDS−urea−PAGE was carried out at 4 °C in the dark as previously described (Irrgang et al., 1988) in combination with the discontinuous buffer system reported in Laemmli (1970). Silver staining was carried out following the protocol of Oakley et al. (1980).

Electroblotting has been performed onto PVDF membranes using the tank buffer described by Towbin et al. (1979). Relative molecular masses of polypeptides have been estimated using a rainbow marker kit (2.5−46 kDa, Amersham). The following antisera were used: polyclonal anti-14 (dilution 1/2000) (Irrgang et al., 1993), monoclonal anti-CP24 (designated as BD7; dilution 1/1000) (Plambeck et al., 1995), monoclonal anti-CP29/CP26 (designated as FC8; dilution 1/1000) (Reuter et al., 1990), and polyclonal anti-22 (1/1000) (Ljungberg et al., 1986). For polyclonal antisera goat anti-rabbit IgG has been used as secondary antibodies in combination with Fast Red/naphtol AS MX phosphate. In case of monoclonal antibodies goat anti-mouse IgG was used with diethylcarbazol/H_2O_2 as coloring reagents.

Steady state fluorescence measurements were performed in 0.1 × 10 × 10 mm^3 glass cuvettes at a chlorophyll concentration of 70 μg/mL in a temperature controlled Helium Flow Cryostat (Optistat, Oxford). Under these conditions distortions of the fluorescence spectra due to self-absorption near the absorption maxima were minimized. Fluorescence spectra (1.5 nm emission slit width, excitation wavelength 435 nm) were measured in a Shimadzu RF-5001PC spectrofluorometer.

Fluorescence decay measurements were performed in the same cuvettes by using a single-photon counting apparatus described previously (Bernarding et al., 1994). The samples were excited at a repetition rate of 4 MHz with 649 nm pulses (FWHM 15 ps), generated by a cavity-dumped dye laser system (Spectra Physics). Fluorescence light of a desired wavelength was selected using a monochromator (1 nm FWHM at low temperature and 4 nm FWHM at room temperature) in combination with a red (>650 nm) cutoff filter and detected by a R1645 U-01 MCP-photomultiplier (Hamamatsu). The response function of the system in this configuration was about 60 ps, as measured with a latex scattering solution. Typically 30 000 counts were collected in the peak channel for the aggregated LHCII samples and 20 000 for their solubilized forms to obtain good signal to noise ratios. In order to unravel the spectral distribution of the emission more than 10 fluorescence decays were measured in the spectral range from 676 to 700 nm for the LHCII samples isolated according to both methods. A set of decays measured at different wavelengths was analyzed using a model function containing several exponential terms convoluted with the system response function. The lifetime of each component was set to be wavelength independent, but the corresponding fractional intensities were permitted to vary as a function of the wavelength. The resulting pre-exponential terms were plotted against the fluorescence emission wavelength to give the decay-associated emission spectra (DAS). The quality of the fit was judged by reduced χ^2, weighted residuals of the fits and the autocorrelation functions.

RESULTS

Steady State Emission Spectroscopy. The fluorescence emission spectrum of the aggregated LHCII prepared according to the method of Burke et al. (1978) was characterized by a maximum at 698 nm and a shoulder near 685 nm when measured at 80 K in a cuvette of 1 mm optical pathway (Figure 1). These results are in close agreement with the data reported for the aggregated LHCII [see Ruban et al. (1995) and references therein]. On the other hand, significantly different spectra were obtained when the same sample has been measured in 0.5 and 0.1 mm cuvettes as is shown

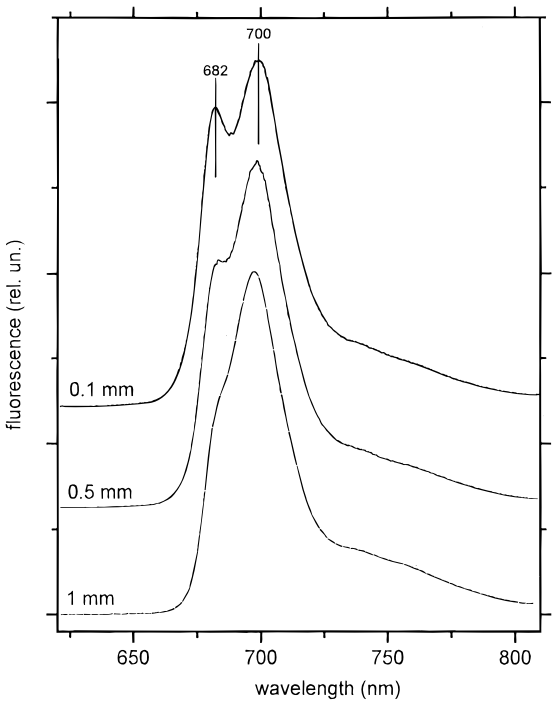

FIGURE 1: Low-temperature (80K) steady state fluorescence emission spectra of the aggregated form of LHCII complexes (Triton X-100 procedure) measured in cuvettes of different optical pathlengths.

in Figure 1. This figure demonstrates that the marked changes of the emission spectrum arise due to a self-absorption near the absorption maxima. As a consequence the ratio between the fluorescence peaks at 682 and 700 nm exhibits a pronounced dependency on the optical pathway. Therefore it is clear that this ratio cannot be used for characterizing the extent of aggregation without considering reabsorption effects. A comparison of the fluorescence spectra of samples at $c_{Chl} = 30$ and 70 μg/mL in a 0.1 mm cuvette revealed that they exhibit nearly the same shape (data not shown). This data shows that the fluorescence spectrum with minimized distortions of reabsorption (Figure 1) is characterized by two peaks at 682 and 700 nm. As a consequence of these findings, subsequent measurements were performed under conditions of negligibly small reabsorption.

The fluorescence emission spectra of solubilized complexes, prepared according to both protocols (Triton X-100 and β-DM procedures) showed narrow peaks near 681 nm (9 nm FWHM) without any shoulder at 700 nm (see Figure 2A) thus indicating that the extent of aggregation was negligible. A FWHM of about 9 nm is very similar to results reported for LHCII from spinach (Hemelrijk et al., 1992) and pea (Kwa et al., 1992) at 77 K. In marked contrast to solubilized trimers did the emission spectrum of aggregated LHCII isolated with β-DM drastically differ from that of the Triton X-100-prepared pigment−protein complexes. Figure 2B reveals that the pronounced band with a maximum at 700 nm characteristic for aggregated Triton X-100-purified LHCII is replaced by only a small shoulder near 690 nm when β-DM-solubilized samples aggregate after dialysis. In both cases, however, large macroaggregates are formed with an average diameter of about 1 μm (the size was determined using laser-scanning fluorescence microscopy, data not shown).

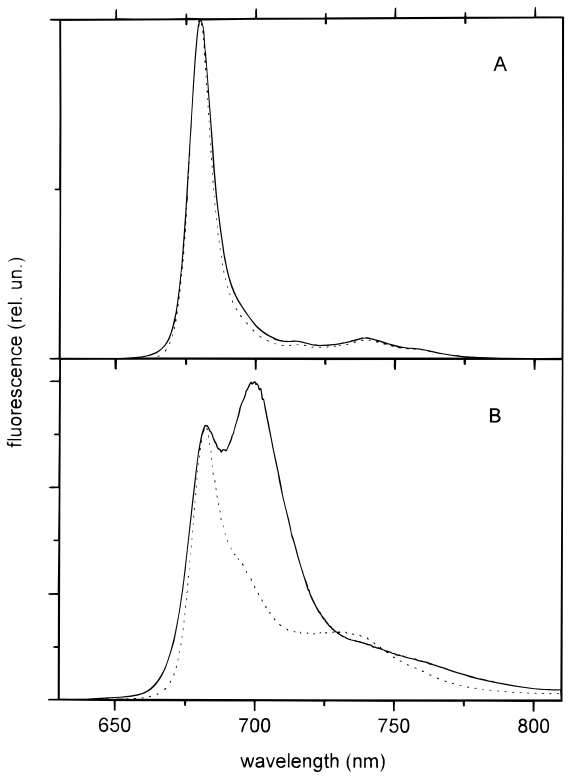

FIGURE 2: Fluorescence spectra of the solubilized (A) and aggregated (B) forms of LHCII complexes prepared by solubilization with β-DM (dashed line) and Triton X-100 (solid line) at temperature 80 K.

In order to exclude the possibility of a trivial effect that might modify the properties of aggregates simply by adding different detergents used for solubilization the following experiments were performed: a sample of β-DM-solubilized LHCII was dialyzed for removing the detergent until complete aggregation was achieved and then divided into two aliquots. One aliquot of the aggregated sample was resolubilized with 0.5% (w/v) Triton X-100 for 30 min at room temperature and dialyzed in order to reform aggregates. The other one was resolubilized in β-DM instead of Triton X-100 using the same procedure as the control experiment. It was found that the fluorescence spectrum of the aggregates obtained after Triton X-100 solubilization did not significantly differ from that of the β-DM-treated samples. Thus, the 700 nm peak characteristic for the aggregated form of LHCII prepared according to Burke et al. (1978) cannot be simply explained by the different type of detergents used for solubilization.

Another possibility to explain the differences between both types of aggregates might be an effect of Ca^{2+}. Ca^{2+} and Mg^{2+} play a role in protein conformation and association of the Chl *a*/*b* binding proteins of the LHCII. Ca^{2+} was found to be tightly bound to the LHCII *in vitro* (Shen et al., 1988a,b; Webber et al., 1989; Irrgang et al. 1991). According to the protocol developed by Burke et al. (1978) the isolation was performed in a cation-free medium and therefore, Ca^{2+} could have been removed from LHCII during this procedure. In contrast to the Triton X-100-purified LHCII, the β-DM-solubilized samples were isolated in a Ca^{2+}-containing buffer and the latter preparations are definitely not deprived of Ca^{2+}. In order to check the possibility of a Ca^{2+}-induced effect β-DM-solubilized LHCII was aggregated in the presence of a chelator using a 10 mM

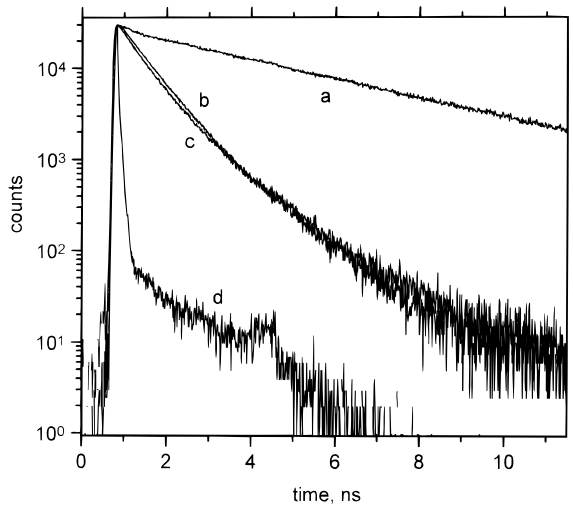

FIGURE 3: Fluorescence decay kinetics of the (a) solubilized and (b) aggregated forms of LHCII complexes prepared with β-DM; (c) fluorescence decay trace of the aggregated form of LHCII prepared using solubilization with Triton X-100; (d) system response function.

EGTA-containing buffer solution in dialysis experiments. The emission spectra of these Ca^{2+}-depleted LHCII aggregates exhibited only a very small fluorescence emission increase in the long-wavelength region compared with aggregates obtained in the absence of the chelator (data not shown). On the basis of these findings it is inferred that neither binding of Ca^{2+} nor the type of detergent (β-DM versus Triton X-100) is critical for the markedly different fluorescence emission spectra of LHCII aggregates prepared by the Triton X-100 or the β-DM procedure (see Figure 2). Accordingly, a more sophisticated mechanism is responsible for this striking feature. It was recently shown that aggregated LHCII obtained from Triton X-100-solubilized samples are characterized by a strong quenching of excited singlet states of Chl *a* (Mullineaux et al., 1993). Therefore both types of LHCII aggregates could have different quenching properties. To address this question time-resolved fluorescence measurements were performed under different conditions.

Fluorescence Decay Kinetics at 277 K. Figure 3 shows decay traces obtained at 277 K in solubilized and aggregated forms of LHCII samples isolated according to the two different isolation protocols described above. The kinetics measured at different wavelengths in the range 675−700 nm were virtually the same (data not shown). This finding indicates that at 277 K rapid Boltzmann equilibration is achieved among all Chl forms within LHCII. Therefore only traces are presented, which have been measured near the fluorescence emission maximum at 682 nm. The kinetic parameters of the fluorescence decay curves obtained in the different preparations used in this study are summarized in Table 1. An inspection of these data readily shows that both types of solubilized LHCII can be described by a biphasic decay kinetics while three exponentials are required for satisfactorily fitting the curves of the aggregated samples. The overall decay of the solubilized preparations is dominated by a 4.3 ns component, which is indicative for the majority of the LHCII preparations in their trimeric state. This result corresponds with those previously reported by Liu et al. (1993). Generally the average fluorescence lifetime significantly decreases down to 0.5−0.8 ns when detergent-solubilized LHCII aggregates. The experimental fluorescence decay is dominated by two kinetics with characteristic lifetimes of 0.2−0.4 and 0.6−0.9 ns for both types of aggregated LHCII, respectively. A minor component with a normalized amplitude of ≤10% exhibits a lifetime of about 2 ns. The 4.3 ns kinetics observed for both Triton X-100- and β-DM-solubilized LHCII completely disappears. Regardless of the kinetic details the data of Table 1 depicts that no significant differences occur between β-DM and Triton X-100 type LHCII under these experimental conditions. This result is in line with previous findings of Gillbro et al. (1988), but markedly shorter lifetimes were reported for a Triton X-100 preparation of aggregated LHCII analyzed by measurements at 80 K (Mullineaux et al., 1993). Despite the latter detail, the measurements at 277 K show that both types of LHCII aggregates exhibit distinct quenching of Chl *a* excited singlet states. Quantitative differences, however, were found for the normalized extent of the fast (0.2−0.4 ns) and middle (0.6−0.9 ns) decay kinetics. The fast kinetics was more pronounced in aggregates obtained from Triton X-100 preparations. In an attempt to analyze these properties in more detail decay-associated emission spectra were measured at low temperatures.

Table 1: Fluorescence Lifetimes and Normalized Amplitudes of Solubilized and Aggregated LHCII (T = 277 K)

solubilized		aggregated	
β-DM	Triton X-100	β-DM	Triton X-100
		22.2% (0.3 ns)	45.1% (0.35 ns)
6.1% (1.9 ns)	8.3% (2 ns)	77.6% (0.75 ns)	57.4% (0.8 ns)
93.9% (4.3 ns)	92.7% (4.5 ns)	0.4% (3 ns)	1.1% (2.4 ns)

DAS of the Solubilized LHCII at Low Temperatures. The global analysis of fluorescence decay curves revealed that a satisfactory fit of the data gathered from measurements with β-DM-solubilized LHCII requires a model function with four exponentials. Figure 4 shows the decay-associated spectra (DAS) recorded at 10 (left side) and 80 K (right side). For comparison the steady state fluorescence emission spectra are also depicted which were measured with the same equipment (not corrected for the spectral sensitivity). The dominating decay component is characterized by a lifetime of 5.4 ns at 80 K and 5.0 ns at 10 K. Similarly to the room temperature measurements a minor component with a lifetime of about 2 ns was also found at 80 and 10 K. The spectral shapes of these two components are almost the same and correspond to the steady state fluorescence emission spectrum.

In contrast to the experiments at 277 K a third decay component with lifetimes in the order of 130−300 ps is observed at low temperatures. The DAS of this component appears to be slightly blue-shifted. At 10 K negative amplitudes are observed.

In the very short time domain a fourth component is observed that is characterized by a negative amplitude in the whole wavelength region. This component could be ascribed to an excitation energy transfer from Chl *b* to Chl *a*. The lifetime of this kinetics is limited by the time resolution of our equipment and is therefore difficult to determine.

DAS of the Aggregated LHCII at Low Temperatures. Figure 5 shows decay associated spectra at 80 K of LHCII aggregates from either Triton-X 100 or β-DM solubilized

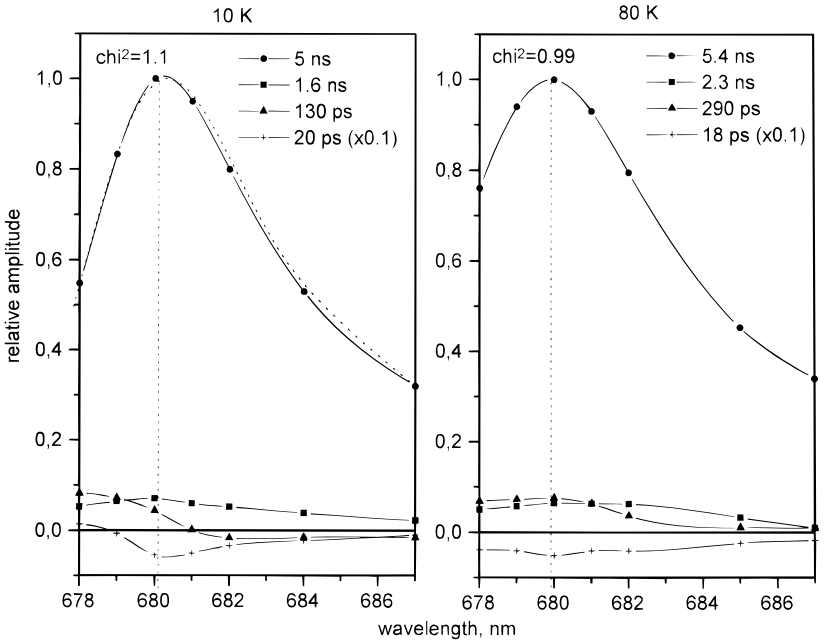

FIGURE 4: DAS measured at 80 and 10 K for solubilized LHCII prepared using the β-DM procedure. The dashed line shows the steady state spectrum.

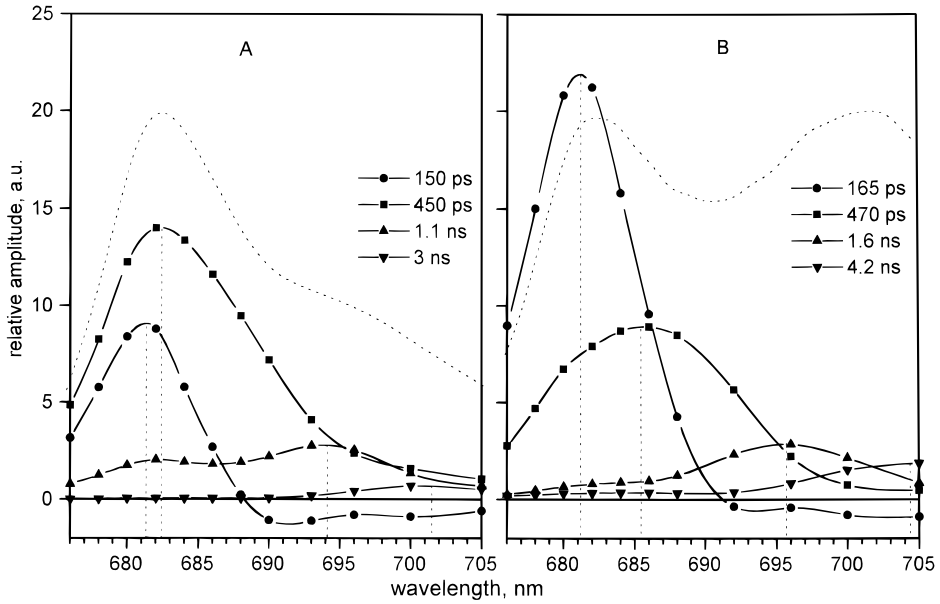

FIGURE 5: DAS measured at 80 K for aggregated LHCII prepared using β-DM (A) and Triton X-100 (B). Steady state emission spectra are shown by the dashed lines.

samples. All DAS were normalized to the sum of the fluorescence yields at the wavelength of the first fluorescence emission maximum (near 682 nm). This is equivalent to the normalization of the steady state fluorescence emission spectra (shown in Figure 5 by the dashed line). An inspection of the data shows that in contrast to the measurements at 277 K several components with different spectral shapes can be resolved at 80 K. This effect is due to a shift of the Boltzmann equilibrium toward the long-wavelength forms of Chl *a*. Both sample types exhibit DAS that comprise four decay components and one rising component with a lifetime of about 15 ps. The latter is attributed to excited state energy transfer from Chl *b* to Chl *a* as in the case of solubilized LHCII. For the sake of a better presentation a component with negative amplitude is omitted in Figure 5 and 6.

The four decay components have similar lifetimes in both samples, but their normalized extents are markedly different. It has to be emphasized that the results obtained with the Triton X-100 preparation are qualitatively in excellent agreement with corresponding data previously reported in the literature (Mullineaux et al., 1993). Therefore, the observed differences between Triton X-100 and β-DM type LHCII aggregates are characteristic features of these samples. The most striking difference is the ratio of the extent of the first and the second component. In the Triton X-100 preparation the 165 ps kinetics dominates the overall decay while in the β-DM type preparation the 450 ps component is the most prominent kinetics (see Figure 5). The DAS of the second component has a maximum at 682 nm in the β-DM type preparation, whereas it is red-shifted by about 3 nm in the Triton X-100−LHCII. The lifetimes of the third

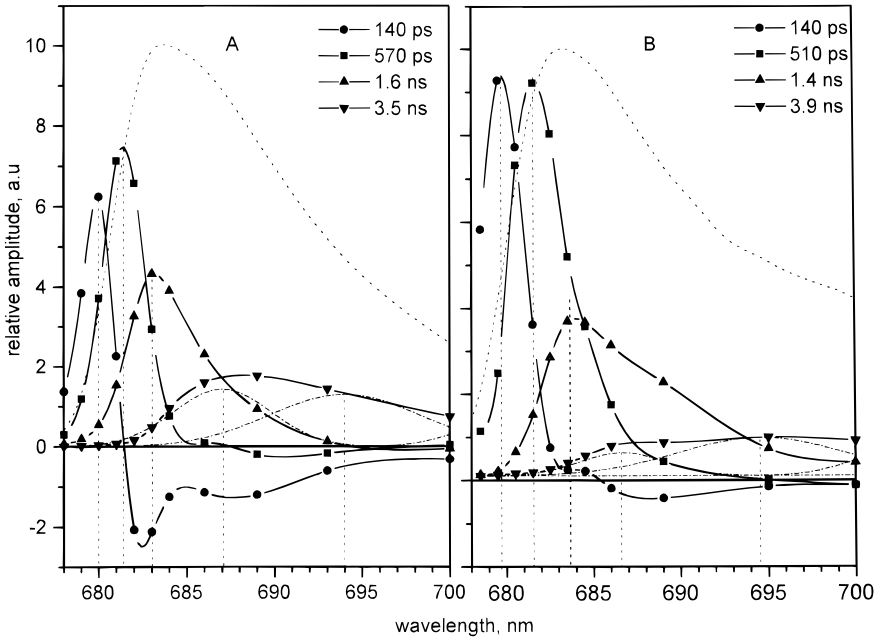

FIGURE 6: DAS measured at 10 K for aggregated LHCII prepared with prepared using β-DM (A) and Triton X-100 (B). Steady state emission spectra are shown by the dashed lines.

and the fourth components are somewhat larger in the Triton X-100 preparation, and they are red-shifted compared with corresponding components of β-DM samples, like the second DAS component. The maximum of the 1.1 (1.6 ns) component is near 695 nm, and a pronounced shoulder at 682 nm is observed in the β-DM type preparation. The normalized extent of the longest lifetime component is 3−4 times larger in the Triton X-100 preparation.

To gather further information on decay constants of different red-shifted Chl emitting species experiments were performed at 10 K, where uphill energy transfer between pigments whose energy levels are shifted by more than 1 nm can be neglected (rate constant of the reverse energy transfer will be a factor of 100 smaller than that of the downhill process) and effects of reabsorption are less pronounced due to the narrowing of the absorption bands. To improve the spectral resolution fluorescence decay kinetics were measured with steps of 1 nm in the range from 678 to 684 nm and at longer wavelength with steps of 2 nm.

The decay associated spectra of the two types of LHCII aggregates at 10 K are depicted in Figure 6. Analogously to the experiments carried out at 80 K five exponential terms are necessary for fitting the data obtained at 10 K. Three narrow components with lifetimes of 140 ps, 510−570 ps, and 1.4−1.6 ns peaking at 680, 681.5, and 683 nm have been found in both types of samples at this temperature. The fourth component is characterized by a maximum around 687 nm and a broad shoulder at the long-wavelength side. The ratio between the 140 and 570 ps components of β-DM type preparation only slightly increases with a decrease of temperature whereas the aggregates of Triton X-100-isolated pigment protein complexes show a pronounced decrease of this ratio. As a consequence of these features the difference between β-DM and Triton X-100 preparations practically vanishes when the temperature is lowered down to 10 K.

To study this effect more precisely we measured the temperature dependency of the fluorescence decay kinetics at 680 nm. Figure 7 presents the normalized amplitudes of the different decay components as a function of temperature. An inspection of this data shows that the temperature dependency for β-DM type preparations exhibits a decrease of the normalized amplitude of the fast decay component and concomitantly an increase of the extent of the 460 ps kinetics. In marked contrast to the β-DM type preparation, the Triton X-100 samples are characterized by an increase of the amplitude of the fast decay and a decrease of the contribution of the 470 ps component. Furthermore, in the Triton X-100 preparation more than half of the temperature effect is accomplished in the range 10 K−30 K whereas in β-DM type samples this effect starts to arise only at $T > 30$ K.

Protein Composition. The polypeptide composition of the Triton X-100- and β-DM-purified LHCII has been analyzed by SDS−urea−PAGE and immunoblotting using a set of antisera directed either against purified minor pigment protein complexes (CP14−15, 22 kDa protein) or monoclonal antibodies recognizing definite epitopes of Chl binding polypeptides (CP24, CP29/CP26) (Ljungberg et al., 1986; Reuter et al., 1990; Irrgang et al., 1993; Plambeck et al., 1995). According to recent results by Funk et al. (1994) the intrinsic 22 kDa polypeptide (*psbS* gene product) binds pigments in contrast to earlier reports (Ljungberg et al., 1986) and was therefore renamed as CP22.

The typical protein composition of LHCII is presented in Figure 8a. The results clearly show that β-DM-solubilized LHCII contains all but one Chl a/b binding polypeptides known to be associated with the antenna system of PSII. Besides the major light-harvesting complex the minor pigment protein complexes CP14−15, CP22, CP24, and CP26 (CP29 type I gene product) have been unambiguously identified whereas CP29 (CP29 type II gene product) which is mainly bound to the PSII core complex was not found in β-DM preparations [for nomenclature see Pichersky et al. (1991) and Jansson (1994)]. In contrast, Triton X-100-purified LHCII was contaminated by a number of not identified polypeptides. This complex was enriched in CP14−15. Additionally we found lower amounts of CP24

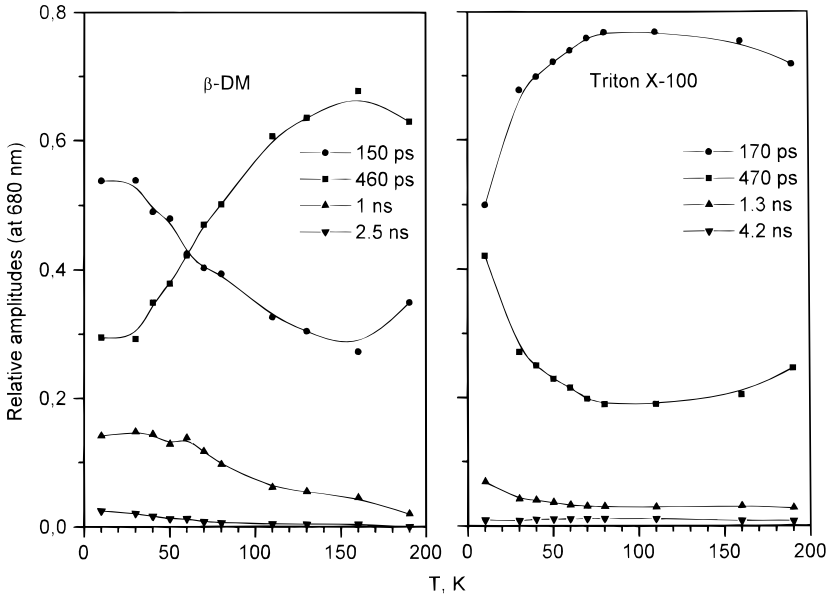

FIGURE 7: Temperature dependency of the normalized amplitudes of fluorescence decay components at 680 nm of LHCII complexes prepared with β-DM (left side) and according to the protocol of Burke et al. (right side).

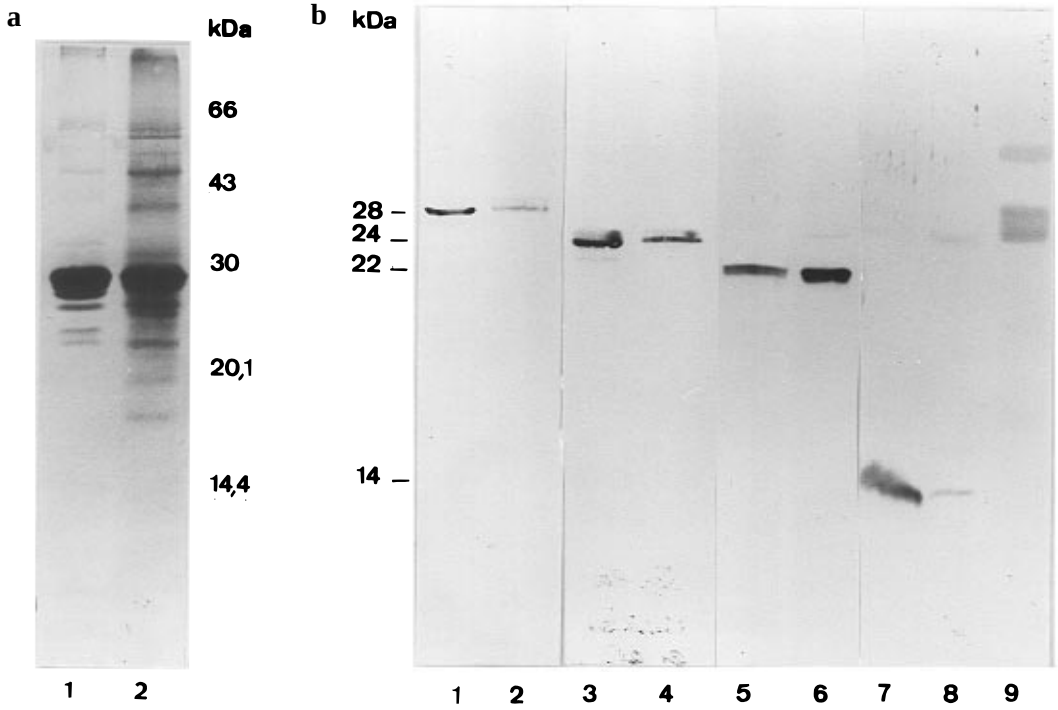

FIGURE 8: (a) SDS−urea−polyacrylamide gel electrophoresis of LHCII. Lane 1: β-DM-solubilized LHCII equivalent to 4 μg of Chl. Lane 2: Triton X-100-solubilized LHCII equivalent to 4 μg of Chl. The polyacrylamide gel was stained with silver. (b) Immunoscreening of β-DM- and Triton X-100-solubilized LHCII. LHCII preparations equivalent to 4 μg of Chl have been separated by SDS−urea−PAGE, electroblotted onto PVDF membranes, and challenged with the following antisera: lanes 1 (β-DM−LHCII) and 2 (Triton X-100−LHCII), anti CP29/26; lanes 3 (β-DM−LHCII) and 4 (Triton X-100−LHCII), anti CP24; lanes 5 (Triton X-100−LHCII) and 6 (β-DM−LHCII), anti 22; lanes 7 (Triton X-100−LHCII) and 8 (β-DM−LHCII), anti CP14/15; lane 9, rainbow marker (46−2.35 kDa). For other details see Materials and Methods.

and only traces of CP 26 (CP 29 type I gene product) in comparison with β-DM solubilized LHCII (see the immunoblot in Figure 8b).

DISCUSSION

The dominating decay component of solubilized LHCII is characterized by a lifetime of 5.4 ns (80 K) and 5.0 ns (10 K). These values are somewhat larger (20−25%) than those of the 4.3 ns component measured at 277 K (see Table 1). This feature of a slight temperature dependency of the lifetime with a maximum near to 80 K is a real effect. A similar phenomenon has been recently reported by Seydack et al. (1995). The normalized extent of this decay component exceeds 90% at all temperatures in the range of 10−277 K. The characteristic temperature dependency of the lifetime very likely originates from slight changes of dissipative decay channels that are less favored at low temperatures whereas the rate constant of the radiative decay as an intrinsic property of the chlorophyll molecule is assumed to be rather independent of temperature. This simple model of thermally

activated radiationless decay, however, does not explain the small but reproducible decrease of the lifetimes when the temperature decreases from 80 K down to 10 K. The origin of this phenomenon remains to be clarified.

The fast (130−300 ps) kinetic component observed in the DAS of solubilized LHCII at low temperatures might reflect an equilibration process between the bulk of Chl *a* emitting at 680 nm and longer wavelength forms as suggested by Mullineaux et al. (1993). It has, however, to be mentioned that in the present study the extent of the fast component is 2−3 times smaller than that of the former report where Triton X-100 type LHCII samples were used. Therefore, the quantitative differences are very likely due to different sample material.

With respect to the origin of the fast kinetics one could speculate that aggregates are formed in a minor fraction of the sample which are characterized by a short lifetime. This interpretation, however, is unlikely if one takes into account that the fluorescence yield of aggregates shows a steeper temperature dependency in the range of 4 K < T < 80 K than that of solubilized LHCII (Ruban et al., 1995a). In this case, the normalized extent of the 0.1−0.3 ns kinetics should markedly increase at 10 K compared with that at 80 K. Figure 4 , however, shows that this is not the case. Therefore, further experiments are required to unravel the nature of this component.

In contrast to the DAS of solubilized LHCII which is characterized by a weak wavelength dependency and a FWHM of about 8 nm due to inhomogeneous line broadening, a pronounced spectral heterogeneity of the fluorescence decay kinetics was observed for aggregated complexes. Two alternative proposals can be offered to explain this heterogeneity of aggregated LHCII observed in the wavelength range of 678−685 nm at 10 K: (1) each of the components (∼140 ps, ∼530 ps, and ∼1.5 ns) originates from a separate ensemble of aggregates with specific quenching properties and spectral shape or (2) all macroaggregates in the sample have very similar properties, but LHCII subunits within an aggregate acquire kinetic heterogeneity due to protein−protein interactions. There are several lines of evidence that the second proposal is more favorable for the following reasons: (i) The relative contributions of the three components were found to be quite similar for aggregates formed either by a long-time dialysis or a rather short procedure, e.g. by adding ethylene glycol as described in [Vasil'ev et al. (1997), data not shown]. The latter procedure yields smaller aggregates and therefore changes of the DAS are expected in the case of the first proposal, if this would be the dominating mechanism. (ii) The steady state emission spectrum is related to the DAS by the expression: $F(\lambda) = \Sigma A_i(\lambda)\tau_i$ with $A_i(\lambda)$ = amplitude of the DAS component and τ_i = lifetime of the corresponding component. Solubilized and aggregated LHCII have the same pigment composition and if the excitonic levels of the pigments are not changed upon aggregation of trimers the relation $A_i(\lambda)$[aggregated] = $A_i(\lambda)$[solubilized] is valid. Decay kinetics of solubilized LHCII at all wavelengths are dominated by a 5 ns component (Figure 4). Therefore with the above mentioned relation the steady state emission spectrum of the solubilized sample is given by: $F(\lambda)$[solubilized] ∼ $\Sigma A_i(\lambda)$[aggregated]. Measured and calculated steady state spectra of solubilized LHCII are in fact very similar (see Figure 9). The first proposal is only coincidentally reconcilable with this finding. In general it is expected that the distribution of the components with lifetimes of about 140 ps, 530 ps, and 1.5 ns will increase inhomogeneous line broadening if each of them would originate from different aggregates. The reconstructed steady state fluorescence emission spectrum of solubilized trimers would be broader than the steady state fluorescence spectrum and its maximum would probably be shifted. As a consequence, the first proposal appears to be very unlikely.

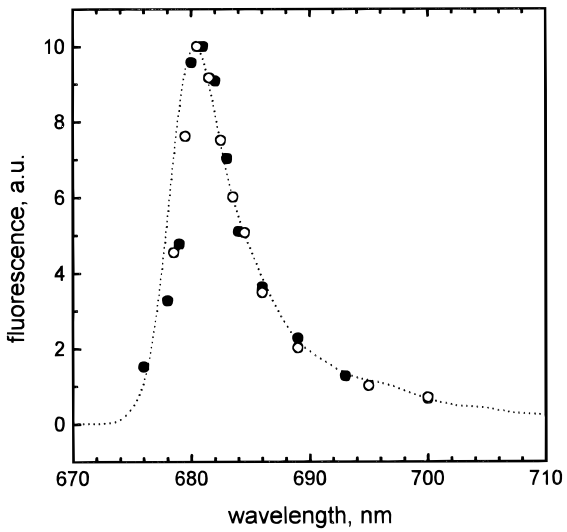

FIGURE 9: Measured steady state spectrum of the solubilized LHCII complexes (dotted line) and steady state spectra of the solubilized LHCII complexes calculated from the DAS of aggregated LHCII prepared using β-DM (solid circles) and Triton X-100 (open circles).

From the measurements performed at 10 K three red-shifted DAS forms were resolved. Two of them are characterized by fluorescence emission maxima and lifetimes of about 681.5 nm (510−570 ps) and 683 nm (1.4−1.6 ns). These forms have a narrow spectral band width, they are similar in both samples, and apparently arise from a heterogeneity of the bulk LHCII. The DAS component with a lifetime of 3.5 ns has a steep slope from the short-wavelength side, its long-wavelength wing spread to a wavelength below 700 nm indicating its composite nature. This component is present in both samples but with a different shape: a smaller contribution in the region from 685 to 695 nm is observed in Triton X-100 samples. Obviously the 3.5 ns component includes a pigment pool with a maximum near 687 nm and several other pools emitting at longer wavelengths. Lifetimes of the red-most species can not be distinguished. In contrast to the situation at 10 K, an uphill excitation energy transfer to the Chl pools with short lifetimes emitting around 680 nm becomes substantially at 80 K according to the Boltzmann law and fluorescence of the pigment pool emitting at 695 nm is diminuished. The DAS forms at 694−696 nm (1.1−1.6 ns) and 702−705 nm (3−4 ns) are clearly observed in both samples at 80 K. In β-DM type samples both components are shifted by about 2 nm to the blue compared with Triton X-100 type LHCII and they have somewhat shorter lifetimes.

Thus, on the basis of the analysis of the DAS measured at 10 K and 80 K for LHCII aggregates five long-wavelength emitting forms were identified that are characterized by maxima at 681.5, 683, 687, 695, and 702 nm. The peak positions of the last four species are in accordance with the recent data obtained from the global deconvolution of the steady state emission spectra at different temperatures (Ruban

et al., 1995a). However, we did not find the DAS component with an emission maximum near 690 nm reported in the latter study probably because its lifetime is close to the lifetime of the 687 nm component.

It has to be emphasized that the interpretation of the experimental data gathered at 80 K in terms of independent emitting species associated with single decay components seems to be rather crude for a description of the time-resolved data obtained with aggregated LHCII at 80 K due to the long-range excitation energy migration observed in macroaggregates (Barzda et al., 1996). At this temperature an uphill energy transfer between pigments with an energy gap of 2−5 nm will be only 2.2−6.6 times slower than the downhill process, and it will lead to a pronounced effect on the decay kinetics. In this case decay rate constants and spectral contours of Chl pools within LHCII aggregates are given by linear combinations of amplitudes and lifetimes of DAS. For example, the contribution of 1.1−1.6 ns decay components in the wavelength region of 680−685 nm can be ascribed to an uphill energy transfer from the Chl pool fluorescing at 695 nm. The 150 (165) ps DAS component at 80 K corresponds to the superposition of the two fast components of the DAS at 10 K which equilibrate at 80 K. The 450 (470) ps DAS component with maxima at 683 nm (β-DM) or 686 nm (Triton X-100) results from the mixing of the DAS forms at 683 and 687 nm observed at 10 K. Unfortunately, model calculations considering the excited state reactions are not possible on the basis of the experimental data of this study. Detailed knowledge of the absorption cross-sections and relative amounts of all Chl pools in LHCII aggregates is required for such an analysis.

Nevertheless, some qualitative conclusions can be drawn from the temperature dependency of fluorescence decay kinetics. The two LHCII preparations exhibit similar decay kinetics at 277 and 10 K in their aggregated forms but they differ significantly at 80 K. The temperature dependency of the two fast components of the β-DM type preparation can be easily explained by line broadening and an increase of the extent of the 450 ps component at 680 nm due to thermal back excitation energy transfer. On the other hand, no simple mechanism can be proposed for a decrease of the extent of the 470 ps component in Triton X-100 type preparations. The temperature effect is already observed at 30 K when line broadening is negligible. The normalized amplitudes of the decay components are affected rather than the corresponding rate constants. These features suggest that decay rates and pathways of energy transfer are similar in both samples, but fractions of pigment pools excited at 650 nm in Triton X-100 type samples are more sensitive to thermal vibrations in the protein matrix than in β-DM-solubilized samples. After excitation at 650 nm energy is transfered to chlorophylls emitting at about 680 nm predominantly via transfer from Chl *b* and Chl a_{676}. We suggest that the rate constants of these steps increase with a temperature rise in Triton X-100 solubilized LHCII, thereby favoring an excitation of the Chl pool with a lifetime of 165 ps. The increase of rate constants can arise from phonon-induced conformational changes of the proteins leading to changes of mutual orientation and/or distances between chromophores.

The DAS of the 140 ps lifetime in the β-DM type preparation crosses the zero level at 681 nm and transforms into a rise component with a maximum between 682 and 683 nm and a shoulder extending to longer wavelengths. This feature would suggest a pronounced energy transfer from the 140 ps to the 570 ps and/or 1.6 ns components. In contrast to the β-DM type preparation, the DAS of the Triton X-100 type preparation shows only a weak rise between 685 and 690 nm.

Recently a detailed spectroscopic analysis has been performed for LHCII preparations that were solubilized with the mild detergent β-DM. It was shown that some spectroscopic properties (e.g. the LD spectrum around 657 nm and the CD spectrum) differ from those observed in LHCII samples isolated by a less gentle treatment, but exhibit strikingly similar spectral features as those observed in intact chloroplasts (Hemelrijk et al., 1992). The results of the present study show that the oligomeric form of LHCII prepared by dialysis of the samples which were isolated by solubilization in β-DM significantly differs in its emission properties from those of aggregates obtained by the Triton X-100 procedure. In addition it is shown that these differences can neither be simply explained by effects due to using a less mild detergent as β-DM nor by effects of bivalent ions like Ca^{2+}. This finding is important because it shows that the mode of interactions between LHCII trimers is very sensitive to some not yet clarified factors.

SDS−urea−PAGE analysis in combination with silver staining and immunoblotting experiments showed that β-DM type LHCII consists of LHCb_1, and LHCb_2 gene products and the minor Chl *a*/*b* binding proteins CP26, CP24, CP22, and CP14/15 (see Figure 8a and b). The Triton X-100-solubilized LHCII contains vanishing amounts of CP26 and about half of the CP24 identified in the β-DM type preparation. The so-called CP14/15 was highly enriched in the Triton X-100 preparation (see Figure 8b). In addition to that is the latter LHCII preparation contaminated with a variety of other not yet identified polypeptides (Figure 8a). As a general feature the Triton X-100-solubilized LHCII revealed a significantly larger statistic variation in its protein composition and fluorescence emission properties than the β-DM type LHCII. Therefore specific spectral and kinetic features of LHCII aggregates could be inferred to be dependent on the presence/absence of an interaction with other polypeptides. The two types of preparations exhibit fluorescence kinetic differences in the wavelength range of the bulk Chl *a*. This effect seems to be in correlation with the extent of the 700 nm fluorescence emission band. Possibly the interaction of the major LHCII with the minor Chl *a*/*b* binding proteins is responsible for both effects giving rise to the 700 nm fluorescence emission band and changing excitonic levels of their neighboring units. It is has to be emphasized, however, that we are not able to unambiguously identify which of the minor Chl *a*/*b* binding proteins being tested is of crucial importance for this specific effect on the amplitude of the 700 nm fluorescence emission band and the temperature dependency of the fluorescence decay.

An alternative possibility to explain differences between the two types of LHCII preparations might be a varying content of phosphorylated LHCII. Compared with the β-DM samples, Triton X-100 LHCII prepared from thylakoids could be enriched in phosphorylated LHCII from stroma membranes. Phosphorylated pigment protein complexes carry negative charges which are in Coulomb interaction with cations and probably protein−protein interactions are also sensitive to the state of phosphorylation. Further experiments

are in progress to clarify this point.

Possible effects of carotenoid and lipid composition also have to be considered as important regulatory factors. It was previously found that the carotenoid composition has no influence on the DAS of aggregates *in vitro* (Mullineaux et al., 1993). Hence, we do not believe that the results of our study can be explained by different carotenoid compositions. Gilmore et al. (1995) showed that fluorescence quenching *in vivo* can be stimulated by xanthophylls but only in presence of ΔpH across the thylakoid membrane. Therefore experiments with more native systems are necessary to clarify this problem. It has been thoroughly investigated that phosphatidylglycerol is not only bound to LHCII (Tremolieres et al., 1981; Remy et al., 1982; Remy et al., 1984) but is also essential for the oligomerization into and stability of the trimeric form (Krupa et al., 1992). Its binding site is not yet completely elucidated but is very likely located between amino acids 9 and 49 of the protein (Nussberger et al., 1993). In addition digalactosyldiacylglycerol is structurally important for the trimer probably located at its periphery (Nussberger et al., 1993). Therefore it is necessary to analyze the lipid content of the two types of samples in their solubilized and aggregated states. We are going to address these questions in our future investigations using samples (e.g. LHCII pigment-proteins reconstituted into lipid vesicles) in which effects of the lipid environment, ΔpH, and carotenoids can be characterized.

In conclusion, the results of the present study show that the spectral properties and the excited state dynamics of LHCII aggregates markedly depend on the molecular composition of the two sample types. Minor Chl *a*/*b* proteins, the lipid composition and/or the extent of protein phosphorylation could modulate their characteristics. The regulatory role of these factors in the native thylakoid membrane remains to be analyzed.

ACKNOWLEDGMENT

We thank B. Lange for excellent technical assistance, and Profs. Andersson and Berg for providing antisera against the 22 kDa protein, CP24 and CP29/26.

REFERENCES

Barzda, V., Garab, G., Gulbinas, V., & Valkunas, L. (1996) *Biochim. Biophys. Acta 1273*, 231−236.
Bassi, R., & Dainese, P. (1992) *Eur. J. Biochem. 204*, 317−326.
Bernarding, J., Eckert, H.-J., Eichler, H.-J., Napiwotzki, A., & Renger, G. (1994) *Photochem. Photobiol. 59*, 566−573.
Burke, J. J., Ditto, C. I., & Arntzen, C (1978) *Arch. Biochem. Biophys. 187*, 252−263.
Du, M., Xie, X., Mets, L., & Fleming, G. R. (1994) *J. Phys. Chem. 98*, 4736−4741.
Funk, C., Schröder, W. P., Green, B. R., Renger, G., & Andersson, B. (1994) *FEBS Lett. 342*, 261−266.
Garab, G., Kieleczawa, J., Sutherland, J. C., Bustamante, C., & Hind, C. (1991) *Photochem. Photobiol. 54*, 273−281.
Gillbro, T., Sandstrom, A., Spangfort, M., Sundstrom, V., & van Grondelle, R. (1988) *Biochim. Biophys. Acta 934*, 369−374.
Gilmore, A. M., Hazlett, T. L., & Govindjee (1995) *Proc. Natl. Acad. Sci. U.S.A. 92*, 2273−2277.
Hemelrijk, P. W., Kwa, S. L. S., van Grondelle, R., & Dekker, J. P. (1992) *Biochim. Biophys. Acta 1098*, 159−166.
Horton, P., Ruban, A. V., Rees, D., Pascal, A. A., Noctor, G., & Young, A. J. (1991) *FEBS Lett. 292*, 1−4.
Horton, P., Ruban, A. V., & Walters, R. G. (1994) *Plant Physiol. 106*, 415−420.
Irrgang, K.-D., Boekema, E. J., Vater, J., & Renger, G. (1988) *Eur. J. Biochem. 178*, 207−217.
Irrgang, K.-D., Renger, G., & Vater, J. (1991) *Eur. J. Biochem. 201*, 512−522.
Irrgang, K.-D., Kablitz, B., Vater, J., & Renger, G. (1993) *Biochim. Biophys. Acta 1143*, 173−182.
Jansson, S. (1994) *Biochim. Biophys. Acta 1184*, 1−19.
Jennings, R. C., Zucchelli, G., Bassi, R., Vianelli, A., & Garlaschi, F. M. (1994) *Biochim. Biophys. Acta 1184*, 279−283.
Krupa, Z., Williams, J. P., Mobashoher, U. K., & Huner, N. P. A. (1992) *Plant Physiol.* 100, 931−938.
Kühlbrandt, W., Wang, D. N., & Fujiyoshi, Y. (1994) *Nature 367*, 614−621.
Kwa, S. L. S., Newell, W., van Grondelle, R., & Dekker, J. P. (1992) *Biochim. Biophys. Acta 1099*, 193−202.
Laemmli, U. K. (1970) *Nature (London) 227*, 680−685.
Liu, B., Napiwotzki, A., Eckert, H.-J., Eichler, H.-J., & Renger, G. (1993) *Biochim. Biophys. Acta 1142*, 129−138.
Ljungberg, U., Akerlund, H.-E., & Andersson, B. (1986) *Eur. J. Biochem. 158*, 477−482.
Mullineaux, C. W., Pascal, A. A., Horton, P., & Holzwarth, A. R. (1993) *Biochim. Biophys. Acta 1141*, 23−28.
Nussberger, S., Dörr, K., Wang, D. N., & Kühlbrandt, W. (1993) *J. Mol. Biol.* 234, 347−356.
Oakley, B. R., Kirsch, D. R., & Morris, N. R. (1980) *Anal. Biochem. 118*, 197−203.
Pichersky, E., Subramanian, R., White, M. J., Reid, J., Aebersold, R., & Green, B. R. (1991) *Mol. Gen. Genet.* 227, 277−284.
Plambeck, C., Reuter, R. A., & Berg, S. P. (1995) in *Photosynthesis: From Light to Biosphere* (Mathis, P., Ed.) Vol. 3, pp 349−352, Kluwer Academic Publishers, Dordrecht, The Netherlands.
Porra, R. G, Thompson, W. A., & Kriedemann, P. E. (1989) *Biochim. Biophys. Acta 975*, 384−394.
Remy, R., Tremolieres, A., Duval, J. C., Ambard- Bretteville, F., & Dubacq, J. P. (1982) *FEBS Lett. 137*, 271−275.
Remy, R., Tremolieres, A., & Ambard-Bretteville, F. (1984) *Photobiochem. Photobiophys. 7*, 267−276.
Reuter, R. A., White, L. A., & Berg, S. P. (1990) in *Current Research in Photosynthesis* (Baltschefsky, M., Ed.) Vol. 1, pp 671−674, Kluwer Academic Publishers, Dordrecht, The Netherlands.
Roelofs, T. A., Lee, C.-H., & Holzwarth, A. R. (1992) *Biophys. J. 61*, 1147−1163.
Ruban, A. V., & Horton, P. (1992) *Biochim. Biophys. Acta 1102*, 30−38.
Ruban, A. V., & Horton, P. (1994) *Photosynth. Res. 40*, 181−190.
Ruban, A. V., Dekker, J. P., Horton, P., & van Grondelle, R. (1995a) *Photochem. Photobiol. 61*, 216−221.
Ruban, A., Horton, P., & Robert, B. (1995b) *Biochemistry 34*, 2333−2337.
Seydack, M., Redlin, H., & Voigt, J. (1995) in *Photosynthesis: From light to Biosphere* (Mathis, P., Ed.) Vol. 1, pp 283−286, Kluwer Academic Publishers, Dordrecht, The Netherlands.
Shen, J.-R., Satoh, K., & Katoh, S. (1988a) *Biochim. Biophys. Acta 933*, 358−364.
Shen, J.-R., Satoh, K., & Katoh, S. (1988b) *Biochim. Biophys. Acta 936*, 386−394.
Towbin, H., Staehelin, T., & Gordon, J. (1979) *Proc. Natl. Acad. Sci. U.S.A. 76*, 4350−4354.
Tremolieres, A., Dubacq, J. P., Ambard-Bretteville, F., & Remy, R. (1981) *FEBS Lett.* 130, 27−31.
van Grondelle, R., Dekker, J. P., Gillbro, T., & Sundstrom, V. (1994) *Biochim. Biophys. Acta 1187*, 1−65.
Vasil'ev, S., Schrötter, T., Bergmann, A., Irrgang, K.-D., Eichler H.-J., & Renger G. (1997) *Photosynthetica 33*, 553−561.
Webber, A. N., & Gray, J. C. (1989) *FEBS Lett. 249*, 79−82.

BI9625253